Fermi National Accelerator Laboratory

FERMILAB-Conf-98/186

Recent Results from the Tevatron

Luc Demortier

Fermi National Accelerator Laboratory
P.O. Box 500, Batavia, Illinois 60510

June 1998

Published Proceedings of the *6th International Workshop on Deep Inelastic Scattering and QCD (DIS 98)*,
Brussels, Belgium, April 4-8, 1998

Operated by Universities Research Association Inc. under Contract No. DE-AC02-76CH03000 with the United States Department of Energy

Disclaimer

Distribution

FERMILAB-Conf-98/186
June 16, 1998
(to be published in DIS98 Proceedings)

RECENT RESULTS FROM THE TEVATRON

LUC DEMORTIER
The Rockefeller University, 1230 York Avenue, New York, NY 10021-6399, USA
E-mail: luc@fnal.gov

We review recent results from fixed-target and collider experiments at the Fermilab Tevatron. Among the topics discussed are jet production rates, α_S measurements, the $\bar{d}/\bar{u}$ ratio in the proton sea, diffraction, heavy quark physics and leptoquark searches.

1 Introduction

The latest Tevatron collider and fixed-target data-taking runs ended in the Fall of 1996 and the Fall of 1997 respectively. The analysis of these datasets is coming to a close, with results ranging from top quark measurements and high-E_T jets to structure functions and diffraction. In this summary we review results that are either new since the last DIS meeting or that remain in disagreement with current theoretical predictions.

2 Tests of QCD

2.1 Inclusive Jet Cross Section

CDF's 1996 measurement of the inclusive jet E_T distribution [1] agrees with next-to-leading order (NLO) QCD predictions over six orders of magnitude, up to a jet E_T of 200 GeV. Above that value, the measurement consistently exceeds the prediction in a way that can not be modelled by the shape of the systematic uncertainties. This trend has recently been confirmed by a new CDF measurement based on an independent sample, 4.5 times larger than the previous one. Both measurements are compared with theoretical predictions in Figure 1. The DØ result, shown in Figure 2, also exceeds the prediction at high-E_T, although not as significantly as the CDF one. A direct comparison of CDF and DØ indicates agreement within the measurement uncertainties (Figure 3). The theoretical calculation itself has several uncertainties (renormalization and factorization scales, clustering algorithm, parton distributions), and a high-E_T excess can easily be accomodated by a modification of the gluon distribution function at high x. Such a modification would not be incompatible with other experimental data entering global parton distribution fits, as demonstrated by the CTEQ collaboration's CTEQ4HJ fit [2].

CDF and DØ have both measured the ratio of inclusive jet cross sections at $\sqrt{s} = 1800$ and 630 GeV, as a function of the dimensionless quantity $x_T \equiv 2E_T/\sqrt{s}$. Several experimental and theoretical uncertainties cancel in this

ratio. As shown in Figure 4, the measurements are consistent with each other, but are approximately 15% below the NLO QCD prediction.

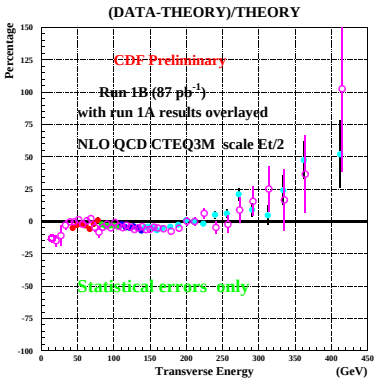

Figure 1: CDF measurements of the inclusive jet E_T spectrum at $\sqrt{s} = 1800$ GeV, for $0.1 < |\eta_{\rm jet}| < 0.7$.

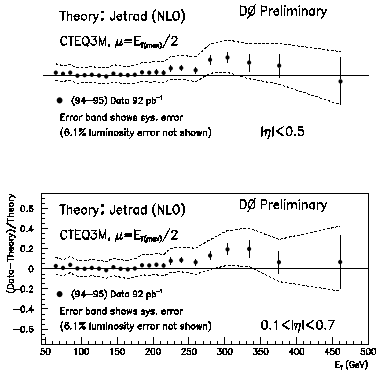

Figure 2: DØ measurements of the inclusive jet E_T spectrum at $\sqrt{s} = 1800$ GeV, for $|\eta_{\rm jet}| < 0.5$ (top) and $0.1 < |\eta_{\rm jet}| < 0.7$ (bottom).

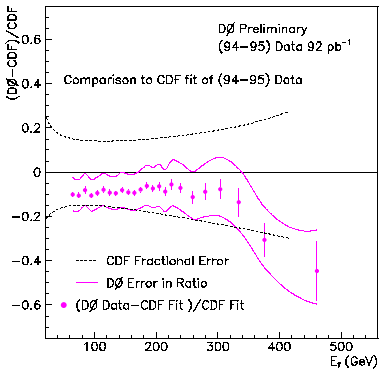

Figure 3: Direct comparison of the measured CDF and DØ inclusive jet E_T spectra at $\sqrt{s} = 1800$ GeV.

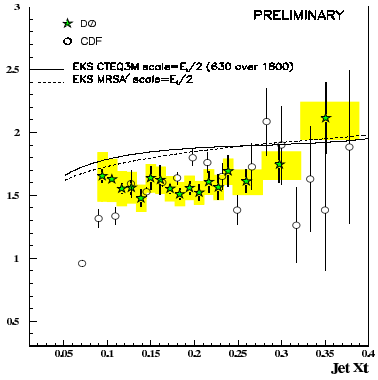

Figure 4: Ratio of the inclusive jet cross section at $\sqrt{s} = 1800$ GeV to that at 630 GeV, as a function of x_T. The shaded areas represent the systematic uncertainty on the DØ result.

2.2 Measurements of the Fraction of W Bosons Produced with Jets

At the previous DIS workshop, DØ reported on a measurement of the ratio of exclusive production cross sections[3] $\mathcal{R}^{10} \equiv \sigma(W + 1\text{jet})/\sigma(W + 0\text{jets})$, and

observed a large discrepancy with NLO QCD predictions. CDF has recently completed a similar analysis[4] by measuring the ratio of inclusive cross sections $\mathcal{R}_{10} \equiv \sigma(W+ \geq 1\text{jet})/\sigma(W)$ as a function of the minimum E_T requirement on the jet. The CDF and DØ measurements are compared to NLO QCD theoretical predictions in Figures 5 and 6. The CDF measurement agrees well

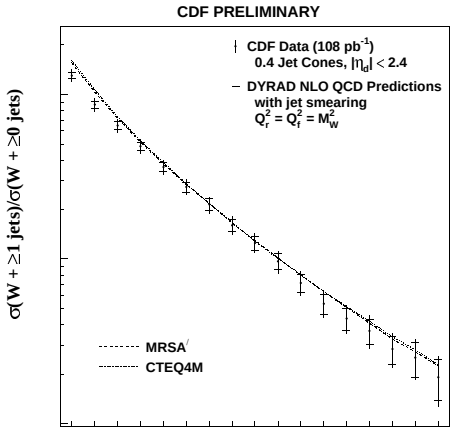

Figure 5: CDF measurement of $\mathcal{R}_{10}$ versus jet E_T threshold, compared to NLO QCD predictions using the MRSA′ and CTEQ4M parton distribution functions. The inner error bars include statistical uncertainties only; the outer error bars include statistical and systematic uncertainties added in quadrature.

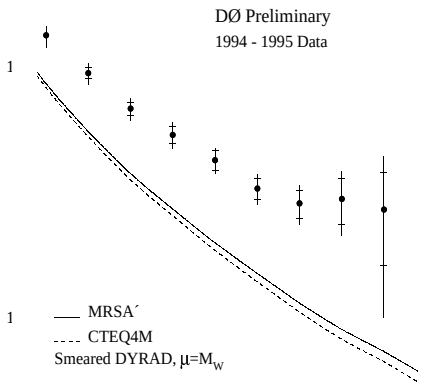

Figure 6: DØ measurement of $\mathcal{R}^{10}$ as a function of the minimum E_T cut on the jet. The data are compared to NLO QCD predictions using the MRSA′ and CTEQ4M parton distribution functions.

with the prediction for $E_T^{\min} > 25$ GeV. At $E_T^{\min} = 0$, the measured value of $\mathcal{R}_{10}$ is 1 by definition, whereas the NLO QCD prediction diverges. In addition there are soft gluon resummation effects at low E_T which are not included in the calculation. Differences between the CDF and DØ analyses include the jet cone radius (0.4 for CDF, 0.7 for DØ) and the fact that the CDF measurement is inclusive, whereas the DØ one is exclusive.

2.3 Extraction of α_s from Jet Data

In $p\bar{p}$ collisions at $\sqrt{s} = 1800$ GeV, the ratio $\mathcal{R}_{10}$ is fairly insensitive to $\alpha_S(M_Z)$ because of a cancellation between contributions from the gluon density evolution and from the hard scattering matrix element [5]. However, CDF has

extracted α_S from the inclusive jet E_T distribution. The method [6] consists of expanding $d\sigma/dE_T$ to NLO in α_S; the E_T dependence of the coefficients of this expansion is obtained from the NLO JETRAD [7] Monte Carlo calculation for a given set of parton distributions and for the appropriate experimental cuts and jet algorithm. Each E_T bin of the measured cross section is then compared with the calculation to produce an independent measurement of $\alpha_S(E_T)$. Using a 2-loop renormalization group equation, $\alpha_S(E_T)$ is subsequently evolved to $\alpha_S(M_Z)$, and an error-weighted average of $\alpha_S(M_Z)$ is performed over the entire E_T range of the measurement. In the end one makes two comparisons: the measured running of $\alpha_S(E_T)$ with QCD predictions that use the extracted average $\alpha_S(M_Z)$, and the extracted average $\alpha_S(M_Z)$ with the input α_S used in the parton distributions. Figure 7 shows the CDF measurement compared to predictions based on the CTEQ4M and CTEQ4HJ parton distributions. The

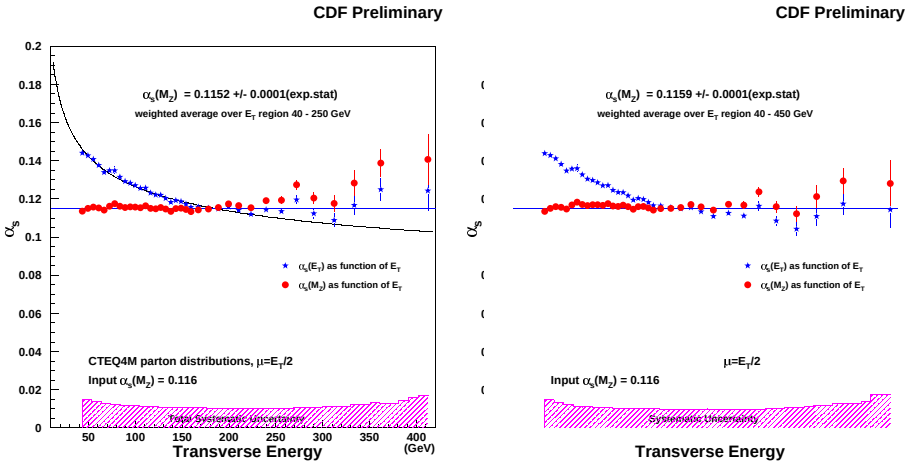

Figure 7: CDF measurement of $\alpha_S(E_T)$ and $\alpha_S(M_Z)$ as a function of E_T for two sets of parton distributions: CTEQ4M (left) and CTEQ4HJ (right).

prediction based on CTEQ4HJ is slightly better, which is expected since the CTEQ4HJ fit gives more weight to the high-E_T points of the CDF inclusive jet data than the CTEQ4M fit [2].

Because the gluon density itself depends on α_S, this measurement is hardly more than a consistency check. Less correlated measurements of α_S and the gluon distribution can be extracted from the dijet triple differential cross section $d^3\sigma/dE_T d\eta_1 d\eta_2$, or even better, from global parton distribution fits.

2.4 FNAL E866/NuSea Results on $\bar{d}/\bar{u}$ Ratio in Proton Sea

Fermilab experiment E866 (NuSea) measured the Drell-Yan dimuon yield from 800 GeV/c protons on hydrogen and deuterium targets [8]. This measurement is sensitive to the ratio of anti-down ($\bar{d}$) to anti-up ($\bar{u}$) quark distributions in the proton sea. The $\bar{d}(x)/\bar{u}(x)$ ratio extracted from the E866 data disagrees with current parton distributions (CTEQ4M, MRSR1) for $x \geq 0.15$, which corresponds to the rapidity at which the CDF W-asymmetry data also start to deviate from current NLO QCD predictions. The CTEQ group has modified the $\bar{d}(x)$ and $\bar{u}(x)$ parameterizations and has incorporated the E866 and CDF data in a new fit [9], to be released as CTEQ5. Figures 8 and 9 show how well the new parameterizations fit the data from both experiments.

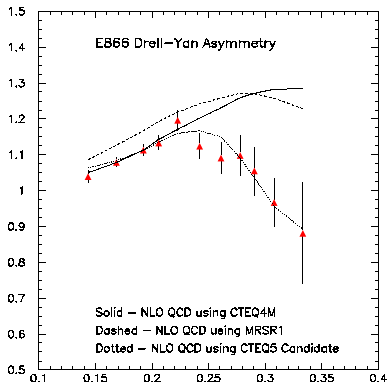

Figure 8: FNAL-E866 measurement of the ratio of the Drell-Yan dimuon cross sections from 800 GeV/c protons on hydrogen and deuterium targets, compared with NLO QCD predictions based on CTEQ4M (solid), MRSR1 (dashed) and CTEQ5 (dotted) parton distributions.

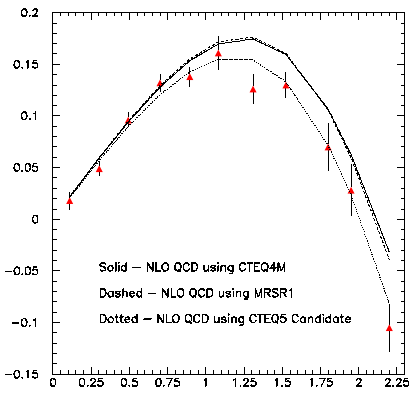

Figure 9: CDF measurement of the W boson charge asymmetry as a function of lepton rapidity, compared with NLO QCD predictions based on CTEQ4M (solid), MRSR1 (dashed) and CTEQ5 (dotted) parton distributions.

It should be noted that the change from CTEQ4 to CTEQ5 has a negligible effect on current measurements of the W boson mass.

3 Diffractive Physics

One of the most interesting new developments at the Tevatron over the last few years is the observation of hard-scattering features in diffractive interactions.

There are two techniques to detect diffraction. The first one relies on the observation of a track from a recoiling beam particle (p or $\bar{p}$) in a spectrometer placed at very small angle with respect to the beam line. The second technique looks for regions of rapidity that are without particles ("rapidity gaps") and therefore signal colorless exchange. CDF makes use of both techniques. It has a Roman Pot spectrometer on one side of the detector to tag recoiling antiprotons and it uses its calorimeter ($|\eta| < 4.2$), central tracking chamber ($|\eta| < 1.8$) and beam-beam counters ("BBC", with $3.2 < |\eta| < 5.9$) to identify rapidity gaps. DØ only works with rapidity gaps, for which it uses calorimetry ($|\eta| < 5.2$), tracking ($|\eta| < 3.5$) and LØ scintillation counters ($1.9 < |\eta| < 4.3$), and has the ability to trigger on rapidity gaps at the hardware trigger level. Experimentally, rapidity gaps are defined as rapidity regions where at least one of the following conditions is met: no hit BBC or LØ counter, no track (with $P_T > 300$ GeV/c for CDF), or no calorimeter tower with energy above some threshold. The following subsections review the current CDF and DØ evidence for three categories of events with rapidity gaps: single diffraction, double-pomeron exchange and color-singlet exchange. The properties of these events are briefly discussed and compared at two different $p\bar{p}$ center-of-mass energies ($\sqrt{s} = 1800$ and 630 GeV) as well as with HERA results.

3.1 Single-Diffractive Dijet and W Boson Production

Single-diffractive events are characterized by a gap in the forward rapidity region of the detector. CDF has found that a fraction [10] $R_W = [1.15 \pm 0.51(\text{stat.}) \pm 0.20(\text{syst.})]\%$ of events with a W boson are diffractive. For dijet events where both jets have $E_T > 20$ GeV, the diffractive fraction [11] is $R_{jj} = [0.75 \pm 0.05(\text{stat.}) \pm 0.09(\text{syst.})]\%$. The ratios R_W and R_{jj} both depend on the gluon fraction f_g inside the pomeron. For example, a high gluon fraction will inhibit diffractive W production and will result in a small value for R_W. By extracting a diffractive structure function from HERA data and assuming factorization of the diffractive cross section, one can predict R_W and R_{jj} as a function of f_g. It turns out that the observed values are lower than the predicted ones by a discrepancy factor D. A simultaneous fit of f_g and D to the observed ratios R_W and R_{jj} yields $f_g = 0.7 \pm 0.2$ and $D = 0.18 \pm 0.04$. The value of f_g agrees with ZEUS measurements, whereas the deviation of D from unity implies a breakdown of the factorization assumption. The value of D can be predicted by introducing a renormalized pomeron flux [12].

The DØ collaboration has measured R_{jj} at two different center-of-mass energies: $R_{jj} = [0.76 \pm 0.04(\text{stat.}) \pm 0.07(\text{syst.})]\%$ at $\sqrt{s} = 1800$ GeV and $[1.11 \pm 0.11(\text{stat.}) \pm 0.20(\text{syst.})]\%$ at $\sqrt{s} = 630$ GeV. Both measurements are

based on events with two jets with $E_T > 12$ GeV and $|\eta| > 1.6$, and with a rapidity gap $2.0 < |\eta| < 4.1$ opposite the dijet system. In contrast with CDF, the DØ measurements are not corrected for the gap detection efficiency. This correction is expected to increase the observed R_{jj} values somewhat, but will not seriously reduce the discrepancy with the HERA measurements.

3.2 Double Pomeron Exchange

Additional information about the structure of the pomeron is obtained by studying pomeron-pomeron collisions ("double pomeron exchange", or DPE for short) that produce dijet events.

At CDF, the pomeron emitted by the antiproton is tagged by a track from the recoiling antiproton in the Roman Pot detector. The pomeron emitted by the proton is tagged by a rapidity gap on the detector side opposite to the Roman Pot. The ratio of the number of dijet events from DPE to that from single diffraction is measured to be[13] $[0.26 \pm 0.05(\text{stat.}) \pm 0.05(\text{syst.})]\%$. This agrees with simulations provided both pomeron fluxes are renormalized by the discrepancy factor D (as defined in section 3.1).

DØ selects dijet events from DPE by requiring a rapidity gap on both sides of a central dijet system[14]. CDF and DØ have analyzed DPE events at both $\sqrt{s} = 630$ GeV and 1800 GeV. Figures 10 and 11 compare the kinematics of DPE events with single-diffractive and non-diffractive events at two different $p\bar{p}$ center-of-mass energies. The jet E_T spectra have the same shape for DPE, single-diffractive and non-diffractive events, hinting at a hard structure for the pomeron.

3.3 Dijet Production by Color-Singlet Exchange

The CDF and DØ collaborations have recently presented evidence for events with a dijet topology where the two jets are separated by a rapidity gap. Although such events indicate the exchange of a color singlet, the underlying physical mechanism is not yet understood and it is not even clear whether it is truly diffractive in origin. Since the rapidity gap occurs in the central region, it can be tagged by studying the multiplicity of both towers above threshold in the calorimeter and tracks in the central tracking chamber.

The DØ evidence is obtained from a sample of events with two jets with $E_T > 12$ GeV, $|\eta| > 1.9$, and pseudo-rapidity separation $\Delta\eta > 4$. Strong gap signals in the region $|\eta| < 1$ are observed at $\sqrt{s} = 1800$ and 630 GeV (see Figure 12). Monte Carlo studies indicate that the particle multiplicities in non-gap events have a negative binomial distribution. This shape is used to subtract the non-gap background in the signal region. The fraction R_{JGJ}

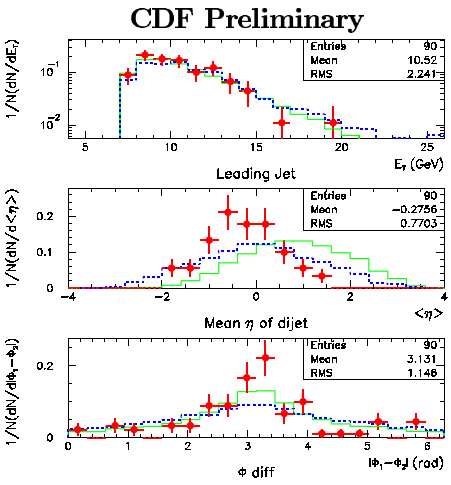

Figure 10: CDF measurement of dijet kinematics at $\sqrt{s} = 1800$ GeV in double-pomeron exchange (data points), single diffraction (dotted histograms) and non-diffractive interactions (dashed histograms). The plots show the leading jet E_T (top), the dijet pseudo-rapidity (middle) and the dijet azimuthal opening (bottom).

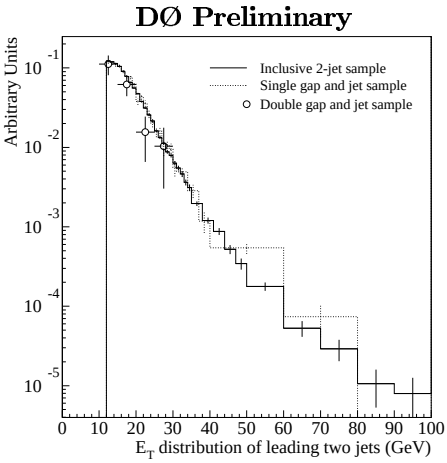

Figure 11: DØ measurement, at $\sqrt{s} = 630$ GeV, of the E_T distributions of the leading two jets for three classes of dijet events: double-pomeron exchange (data points), single diffraction (dotted histogram) and inclusive dijets (solid histogram).

of gap events is measured to be [15] $[1.85 \pm 0.38]\%$ at $\sqrt{s} = 630$ GeV and $[0.54 \pm 0.17]\%$ at $\sqrt{s} = 1800$ GeV. The ratio of the 630 GeV measurement over the 1800 GeV one is 3.43 ± 1.29.

The CDF analysis requires two jets with $E_T > 20$ GeV and $|\eta| > 1.8$. The tower and track multiplicities in the central region of the detector are plotted for two classes of dijet events: those with jets on opposite sides (OS) of the central region, and those with jets on the the same side (SS). The excess of OS over SS events in the low-multiplicity bins is attributed to colorless exchange (see Figure 13). At $\sqrt{s} = 1800$ GeV, the fraction of colorless exchange dijet events is measured to be [16] $R_{JGJ} = [1.13 \pm 0.16]\%$. A similar analysis was repeated at $\sqrt{s} = 630$ GeV, with a lower cut on the jet E_T (8 GeV instead of 20 GeV). There, a preliminary measurement yields [17] $R_{JGJ} = [2.3 \pm 1.0]\%$, so that the ratio $R_{JGJ}(\sqrt{s} = 630\,\mathrm{GeV})/R_{JGJ}(\sqrt{s} = 1800\,\mathrm{GeV})$ is found to be 2.0 ± 0.9, consistent with the DØ measurement.

The structure and couplings of the exchanged color-singlet can be studied by measuring the ratio R_{JGJ} as a function of the dijet E_T and pseudo-rapidity separation $\Delta\eta$, and the $p\bar{p}$ center-of-mass energy $\sqrt{s}$. For example, if the

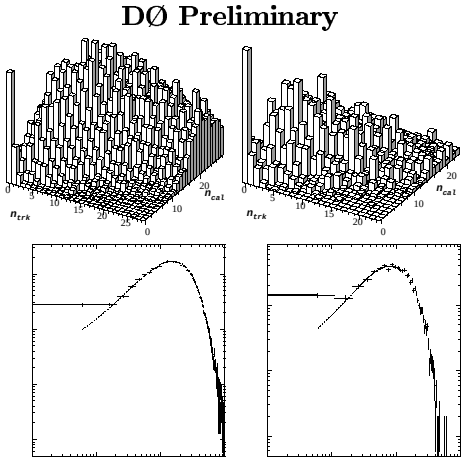

Figure 12: DØ dijet data used for the color singlet exchange studies at $\sqrt{s} = 1800$ GeV (left) and 630 GeV (right). The top plots show distributions of track multiplicity versus calorimeter tower multiplicity in the region $|\eta| < 1$. The excess in the (0,0) bin is attributed to color-singlet exchange. The two bottom plots are histograms of the calorimeter multiplicity. The dashed lines are fits of the leading edges of the distributions to negative binomials and are used as estimates of the non-gap background.

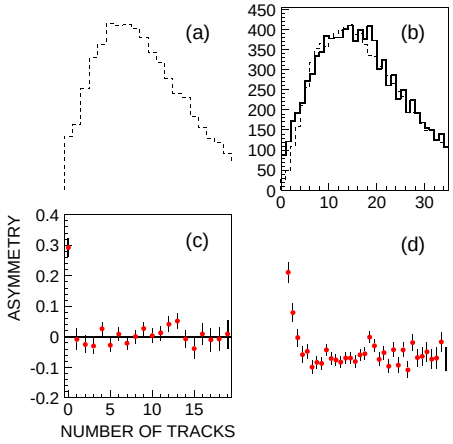

Figure 13: CDF dijet data used for the color singlet exchange study at $\sqrt{s} = 1800$ GeV. The top plots show the tracking multiplicity and the calorimeter tower multiplicity in the central region of the detector for events with jets on opposite sides of this region (solid line), and for events with jets on the same side of this region (dashed line). The bottom plots show the asymmetry (bin-by-bin difference over sum) between the solid and dashed distributions in the top plots. The large asymmetry at low multiplicity is attributed to color-singlet exchange.

color singlet couples more strongly to quarks than gluons, R_{JGJ} will increase as the proportion of quark-initiated processes increases, i.e. with increasing dijet E_T or $\Delta\eta$, and with decreasing $\sqrt{s}$. The DØ measurements (Figure 14) show a slight increase of R_{JGJ} as a function of dijet E_T and $\Delta\eta$, although the uncertainties are still quite large. On the other hand, the CDF data (Figure 15) appear to be flat.

4 Heavy Quark Physics

4.1 Discovery of the B_c Meson

The CDF collaboration recently announced the discovery of the last meson predicted by the standard model, the B_c, in the channel $B_c^{\pm} \to J/\psi \ell^{\pm} X$, where $\ell = e$ or μ, and $J/\psi \to \mu^+\mu^-$. The analysis[18] requires the three leptons μ^+,

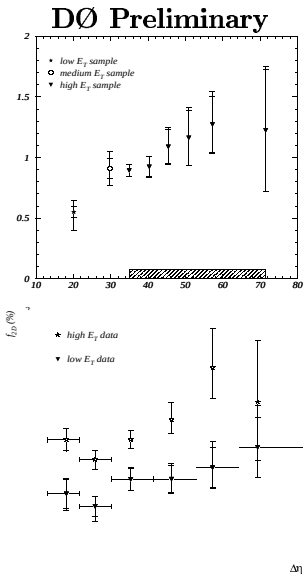

Figure 14: DØ measurements (at $\sqrt{s} = 1800$ GeV) of the fraction of color-singlet events as a function of dijet E_T (top) and $\Delta\eta$ (bottom).

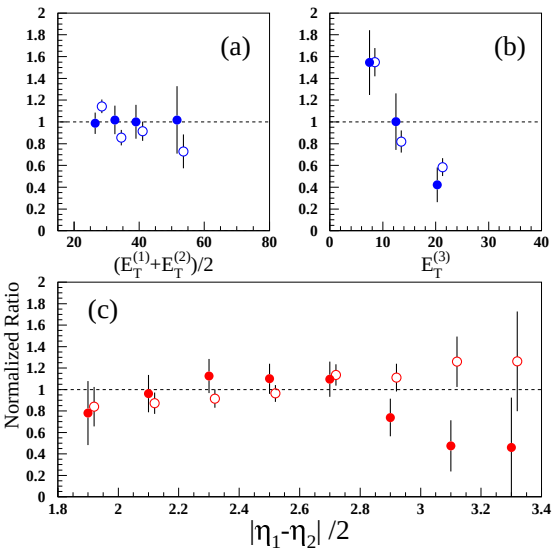

Figure 15: CDF measurements (at $\sqrt{s} = 1800$ GeV) of the fraction of color-singlet dijet events (black circles) as a function of dijet E_T (top left), third jet E_T (top right), and dijet $\Delta\eta$ (bottom). The open circles are for a control sample of events with low (but non-zero) multiplicity between the jets.

μ^- and ℓ to form a good common vertex and removes prompt J/ψ's by cutting on the pseudo-proper decay length $ct^* \equiv L_{xy} \times m(J/\psi\ell)/p_T(J/\psi\ell) > 60$ μm, where L_{xy} is the distance between the event vertex and the B_c decay vertex projected onto a plane perpendicular to the beam direction and projected along the B_c direction in that plane. Since there is a neutrino among the decay products of the B_c, the B_c mass cannot be fully reconstructed. Instead, one forms the invariant mass of the J/ψ and the lepton ℓ and defines the signal region by $4 < m(J/\psi\ell) < 6$ GeV/c^2. The distribution of this mass for the data is compared to signal and background predictions in Figure 16. The probability for a statistical fluctuation in the background to have caused the excess of data is estimated to be 6.3×10^{-7}, which corresponds to 4.8 standard deviations for a Gaussian distribution. A B_c mass measurement is extracted from the $m(J/\psi\ell)$ distribution and yields $M(B_c) = 6.40 \pm 0.39(\text{stat.}) \pm 0.13(\text{syst.})$ GeV/c^2. Figure 17 shows a distribution of the pseudo-proper decay length ct^*,

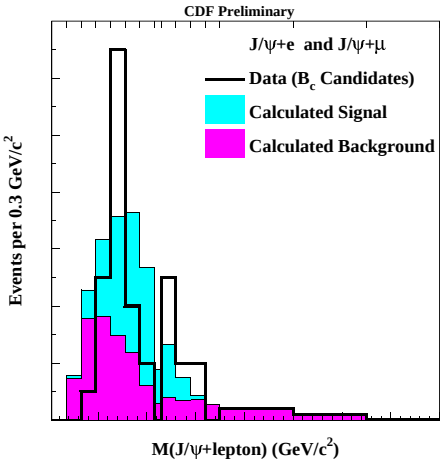

Figure 16: $J/\psi\ell$ invariant mass distribution used for the CDF B_c search and mass measurement. The data are superimposed on the result of the fit to signal + background.

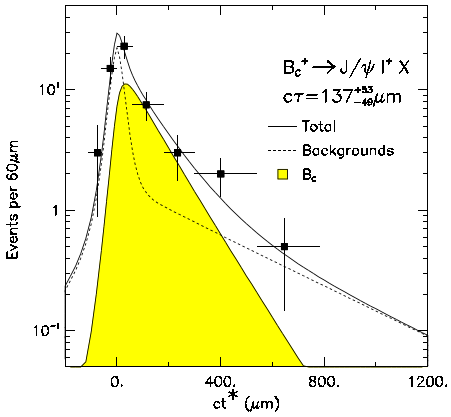

Figure 17: Distribution of the pseudo-proper decay length ct^* with the result of the B_c lifetime fit.

from which the B_c lifetime is measured to be $0.46^{+0.18}_{-0.16}(\text{stat.}) \pm 0.03(\text{syst.})$ ps. CDF has measured the cross section ratio:

$$\frac{\sigma(B_c)\mathcal{B}(B_c \to J/\psi\ell\nu)}{\sigma(B_u)\mathcal{B}(B_u \to J/\psi K)} = 0.132^{+0.041}_{-0.037}(\text{stat.}) \pm 0.031(\text{syst.})^{+0.032}_{-0.020}(\text{lifetime}).$$

Systematic uncertainties due to luminosity, J/ψ trigger efficiency, and track reconstruction efficiency cancel in this ratio.

4.2 Lifetime Measurements, $B^0\bar{B}^0$ Oscillations

CDF has obtained new B hadron lifetime measurements, both from fully reconstructed exclusive B decays and from partially reconstructed inclusive decays. Results from both types of analysis were combined and are summarized in Figure 18.

An examination of the decay length distribution for the B_s^0 meson has led to a limit on the fractional difference in decay width between the two mass eigenstates of B_s^0: $\Delta\Gamma/\Gamma < 0.81$ at the 95% C.L. If $\Delta\Gamma/\Gamma$ turns out to be large enough (of order 20%), it may be possible to measure the angle γ in the unitarity triangle of the CKM matrix by studying CP violation in B_s decays.

Several CDF results on $B^0\bar{B}^0$ oscillations are summarized in Figure 19. Although the scope of this review does not allow a detailed description of each

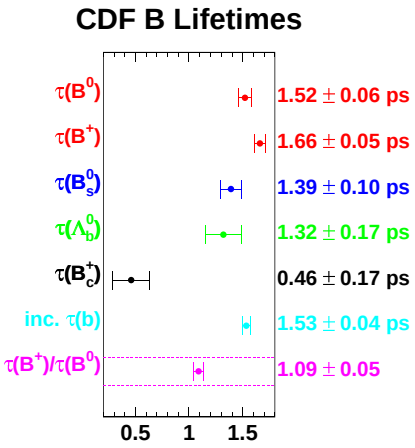

Figure 18: Summary of B hadron lifetimes measured by CDF

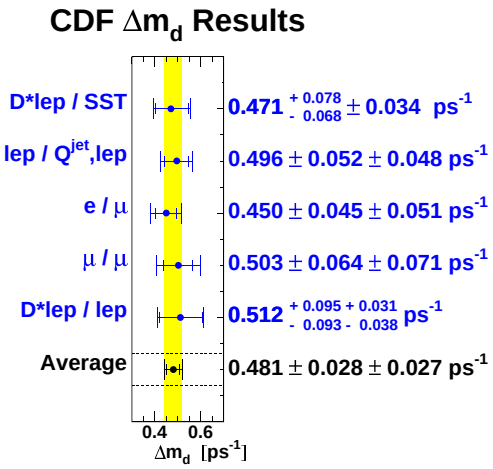

Figure 19: Summary of CDF $B^0\bar{B}^0$ oscillation results.

result, mention should be made of the same-side tagging technique (SST), whereby the flavor of the B meson at production is determined from the charge of nearby particles. This is the most efficient flavor tag found so far and will have significant applications in future studies of CP violation in B decays.

4.3 Inclusive Forward b Production

DØ has studied forward b production by selecting events with a muon with momentum smaller than 150 GeV/c, transverse momentum greater than 2 GeV/c, and pseudo-rapidity between 2.4 and 3.2. The fractions of muons from b- and c-quark decay are estimated from QCD predictions. The unfolded p_T spectrum of forward muons from b decay is compared to NLO QCD in Figure 20. The measured cross section is about four times higher than the NLO QCD prediction.

5 Electroweak Physics

A new and still preliminary measurement of the electroweak mixing angle in νN scattering by the NuTeV experiment [19] yields $\sin^2\theta_W^{(\mathrm{on-shell})} = 0.2253 \pm 0.0019(\mathrm{stat.}) \pm 0.0010(\mathrm{syst.})$. The W-boson mass extracted from this measurement is listed together with CDF and DØ results on M_W and M_{top} in table 1. The current Higgs mass constraints implied by these measurements are shown

Source	M_W (GeV/c^2)	$M_{\rm top}$ (GeV/c^2)
CDF average	80.38 ± 0.12 *	175.3 ± 6.3 *
DØ average	80.43 ± 0.11	172.1 ± 7.1
Hadron collider average	80.40 ± 0.09 *	173.9 ± 5.0 *
NuTeV	80.26 ± 0.11 *	
Lep II	80.35 ± 0.09	
World average	80.345 ± 0.055 *	

Table 1: Measurements of the W-boson mass and the top quark mass as of June 11, 1998. Values marked with a $*$ are preliminary.

in Figure 21.

6 New Phenomena

There is an impressive list of Tevatron searches for evidence of physics beyond the standard model: leptoquarks, magnetic monopoles, quark substructure, supersymmetry, charged Higgs, heavy gauge bosons and more. In general the data are found to be well described by standard model background calculations and are used to derive constraints on various theoretical models.

Table 2 shows the most recent CDF and DØ lower limits on scalar leptoquark masses, as a function of leptoquark generation and branching fraction β into charged lepton plus quark. These limits were obtained by first deriving 95% C.L. upper limits on the leptoquark production cross section as a function of mass, and then finding the mass value where this curve meets a lower bound on the theoretical calculation of the production cross section. DØ has

Leptoquark		95% C.L. lower limit on mass (GeV/c^2)	
Generation	β	(DØ)	(CDF)
1	1.0	225	213
1	0.5	204	180
2	1.0	184	195
2	0.5	140	147
3	1.0	98	99

Table 2: Tevatron results from scalar leptoquark searches.

also obtained 95% C.L. lower limits on the mass of a first-generation vector leptoquark. These limits are 200, 329 and 340 GeV/c^2 for $\beta = 0.0$, 0.5 and 1.0 respectively.

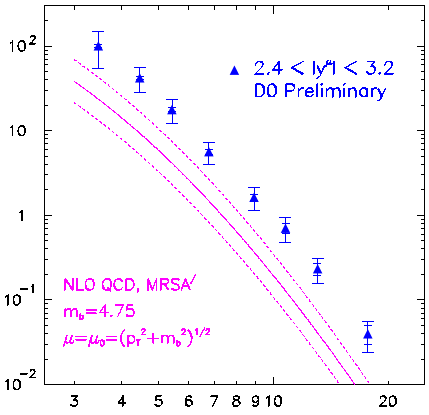

Figure 20: DØ measurement of the unfolded p_T spectrum of forward muons from b decays, compared to NLO QCD predictions.

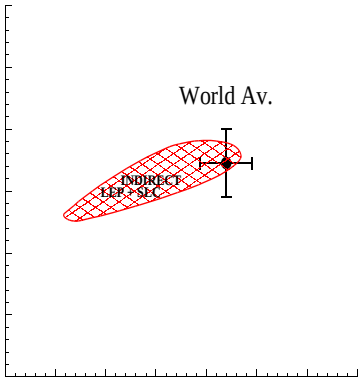

Figure 21: A measurement of $M_{\rm top}$ determines the radiative corrections needed to calculate M_W from M_Z, up to effects involving the Higgs mass. The plot shows how the three masses are related, together with the current world average measurements of M_W and $M_{\rm top}$.

In April 1995 CDF observed an event with missing transverse energy, two photons and two electrons. The probability for this event to come from standard model sources is extremely low, which has prompted a great deal of theoretical speculation, in particular with supersymmetric models. Further experimental searches within the frameworks of these models have all yielded zero result.

7 Conclusions

The Tevatron data have produced a wealth of physics results on a wide variety of processes. In general these results demonstrate a remarkable consistency of the standard model. Wherever there is a discrepancy between measurements and theory, it can either be attributed to a lack of constraints on the theoretical assumptions (e.g. parametrizations of the parton distributions), or to a lack of understanding of how to perform calculations near the boundary of the theory's applicability (e.g. diffractive physics, b production). Except perhaps for one mysterious event observed by the CDF collaboration, there is as yet no sign of new physics.

Acknowledgments

I would like to thank my Tevatron colleagues who helped with the preparation of this review, and especially Anwar Bhatti, Kerstin Borras, Andrew Brandt, Dino Goulianos, Joey Huston, Mike Leitch, Jill Perkins, Heidi Schellman, Greg Snow and Barry Wicklund. I also would like to thank all the organizers for their friendly help and a very interesting workshop.

References

1. F. Abe *et al.*, CDF Collaboration, Phys. Rev. Lett. **77**, 438 (1996).
2. H.L. Lai *et al.*, Phys. Rev. D**55**, 1280 (1997).
3. T.M. Joffe-Minor for the DØ and CDF collaborations, *QCD Studies with W/Z Events at the Tevatron*, 5th International Workshop on Deep Inelastic Scattering and QCD, Chicago, IL, April 1997.
4. F. Abe *et al.*, CDF Collaboration, *Measurement of the* $\sigma(W+ \geq 1\text{Jet})/\sigma(W)$ *Cross Section Ratio from* $p\bar{p}$ *Collisions at* $\sqrt{s} = 1.8$ *TeV*, submitted to Phys. Rev. Lett.
5. S. Abachi *et al.*, DØ Collaboration, Phys. Rev. Lett. **75**, 3226 (1995).
6. W.T. Giele, E.W.N. Glover, and J. Yu, Phys. Rev. D**53**, 120 (1996).
7. W.T. Giele, E.W.N. Glover and D.A. Kosower, Phys. Rev. Lett. **73**, 2019 (1994).
8. E.A. Hawker *et al.*, FNAL E866/NuSea Collaboration, Phys. Rev. Lett. **80**, 3715 (1998).
9. W.K. Tung for the CTEQ Collaboration, *Recent Advances in Global QCD Analysis of Parton Distributions*, 1998 LHC Theory Workshop (unpublished).
10. F. Abe *et al.*, CDF Collaboration, Phys. Rev. Lett. **78**, 2698 (1997).
11. F. Abe *et al.*, CDF Collaboration, Phys. Rev. Lett. **79**, 2636 (1997).
12. K. Goulianos, Phys. Lett. B**358**, 379 (1995).
13. K. Borras for the CDF Collaboration, *Results on Hard Diffraction from CDF*, WG 2, this conference.
14. R. Hirosky for the DØ Collaboration, *Jet Production with Two Rapidity Gaps at DØ* , WG 2, this conference.
15. A. Goussiou for the DØ Collaboration, *Probing Hard Color Singlet Exchange at DØ* , WG 2, this conference.
16. F. Abe *et al.*, CDF Collaboration, Phys. Rev. Lett. **80**, 1156 (1998).
17. K. Borras for the CDF Collaboration, *Results on Dijets with a Central Rapidity Gap from CDF*, WG 2, this conference.
18. F. Abe *et al.*, CDF Collaboration, preprint hep-ex/9805034.
19. K.S. McFarland *et al.*, NuTeV Collaboration, preprint hep-ex/9806013.